DOI: 10.1002/ejoc.200700484

Synthesis, X-ray Crystal Structures and Solid-State Fluorescence Properties of 3-Dibutylamino-6-alkoxy-6-phenylnaphtho[2,3-*b*]benzofuran-11(6*H*)-one Derivatives[‡]

Yousuke Ooyama,*[a] Toshiki Mamura,[a] and Katsuhira Yoshida*[a]

Keywords: Fluorescent dyes / Solid-state fluorescence / Crystal structures / π–π Interaction / Substituent effects

Novel heterocyclic fluorophores – 6-alkoxy-3-dibutylamino-6-phenylnaphtho[2,3-*b*]benzofuran-11(6*H*)-ones **2a**–**2g** with different chain lengths in alkoxy substituents non-conjugatedly linked to the chromophore skeleton – have been derived from the quinol-type compound **1**, and their photophysical properties have been investigated in solution and in the solid state. In solution, the fluorophores **1** and **2a**–**2g** exhibit similar fluorescence properties. In the solid state, however, the fluorophores **2a**–**2g** exhibit stronger fluorescence properties than the quinol **1**. Furthermore, the fluorescence quantum yields (Φ) of **2** in the solid state are higher than those of **2** in solution, and considerable differences in the solid-state fluorescence were observed among the alkoxy derivatives **2a**–**2g**. To elucidate the dramatic effect of the alkoxy substituents we performed semiempirical molecular orbital calculations (AM1 and INDO/S) and X-ray crystallographic analysis. On the basis of the results of the calculations and the X-ray crystal structures, the relationships between the solid-state photophysical properties and the chemical and crystal structures of **1** and **2a**–**2g** are discussed. It was confirmed that the introduction of long alkoxy chains such as butoxy and pentoxy groups in non-conjugated linkage to the chromophore can efficiently prevent short π–π contacts between the fluorophores in molecular aggregation states and thus cause dramatic solid-state fluorescence enhancements.

Introduction

During the last decade there has been a gradual accumulation of information relating to solid-state fluorescence of organic fluorophores, a subject of great interest to the optoelectronics industry in contexts such as light-emitting diodes[1] and photoelectric conversion.[2] Some studies suggested that the key point in the designing of new organic fluorescent dyes exhibiting strong solid emission properties is the removal of the intermolecular interactions between fluorophores that cause fluorescence quenching in molecular aggregation states. For example, the introduction of bulky substituents into the original fluorophores[1f,1j,3,4] and the construction of nonplanar structures containing sterically hindered substituents[4d,5] are known to be very useful methods for solving the problem of fluorescence quenching by aggregation. However, it is difficult to perform a systematic study to investigate the relationship between chemical structures and solid-state emission properties for the appearance of strong solid-state fluorescence of organic fluorescent dyes.

In our previous paper[6] we reported the solid-state fluorescence properties of the novel benzofurano[3,2-*b*]naphthoquinol-type fluorophore **1** and its alkoxy derivative **2b**, with a butoxy substituent in non-conjugated linkage to the chromophore (Scheme 1). Dramatic substituent effects on the solid-state photophysical properties were observed and elucidated by X-ray crystallographic analysis. It was confirmed that the introduction of a butoxy substituent in non-conjugated linkage to the chromophore can efficiently prevent short π–π contacts between the fluorophores in molecular aggregation states and thus cause a dramatic solid-state fluorescence enhancement. This observation suggests that the solid-state fluorescence of the fluorophore is significantly dependent on the steric factors associated with the alkoxy substituent in non-conjugated linkage to the chromophore skeleton at the 6-position in **2**. Here we report the photophysical properties, both in solution and in the crystalline state, of such heterocyclic fluorophores – 6-alkoxy-3-dibutylamino-6-phenylnaphtho[2,3-*b*]benzofuran-11(6*H*)-ones **2** – with different chain lengths in their alkoxy substituents. To elucidate the steric effects of the alkoxy substituents on the solid-state fluorescence excitation and emission spectra, we have performed X-ray crystallographic analyses.

[‡] Heterocyclic Quinol-type Fluorophores, 6. Part 5: Y. Ooyama, T. Okamoto, T. Yamaguchi, T. Suzuki, A. Hayashi, K. Yoshida, *Chem. Eur. J.* **2006**, 12, 7827–7838.

[a] Department of Material Science, Faculty of Science, Kochi University,
Akebono-cho, Kochi 780-8520, Japan
Fax: +81-88-844-8359
E-mail: kyoshida@cc.kochi-u.ac.jp
yooyama@hiroshima-u.ac.jp

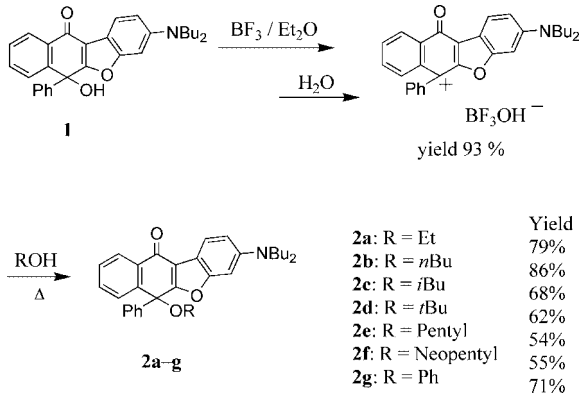

Scheme 1. Synthesis of **2**.

Results and Discussion

Synthesis of 6-Alkoxy-3-dibutylamino-6-phenylnaphtho-[2,3-*b*]benzofuran-11(6*H*)-one Fluorophores 2a–2g

It is known that dialkylamino-substituted triphenylcarbinol analogues undergo dehydroxylation under acidic conditions to give triaryl carbocation salts.[7] In order to prepare alkoxy derivatives of the quinol, we investigated the dehydroxylation of quinol **1**. Treatment of **1** with boron trifluoride in diethyl ether (BF_3·OEt_2) gave the cationic salt in 93% yield (Scheme 1). The cationic salt was then dissolved in alcohols with heating to give the corresponding alkoxy derivatives **2a**–**2g** in high yields (54–86%).

Spectroscopic Properties of 1 and 2 in Solution

The visible absorption and fluorescence spectroscopic data for compounds **1** and **2** in various solvents are summarized in Table 1. The fluorescence spectra of the compounds were recorded by excitation at the wavelengths of the longest absorption maximum. Because of the non-conjugated linkage of the alkoxy and hydroxy groups to the chromophore skeleton, the absorption and fluorescence spectra of the fluorophores **1** and **2** resemble one another very closely. The quinol **1** exhibits two distinct absorption bands at around 391 and 321 nm in benzene, with a weak fluorescence band at around 540 nm (Φ = 0.056). The effect of solvent polarity on the absorption spectrum of **1** is small, whereas its effect on the fluorescence spectrum is large: an increase in solvent polarity causes a large bathochromic shift and a drastic decrease in the fluorescence intensity. The fluorescence intensities in acetonitrile and 95% ethanol were too weak to allow determination of the maximum wavelengths and the quantum yields. The Stokes shift values for **1** are large, even in a solvent of low polarity. The absorption spectra of **2** are little affected by increasing solvent polarity, while their fluorescence spectra show large bathochromic shifts and reductions in fluorescence intensity. The photophysical properties of **2** were similar to those of the quinol **1**.

Semiempirical MO Calculations (AM1, INDO/S)

The photophysical spectra of **1** and **2** were analyzed by semiempirical molecular orbital (MO) calculations. The molecular structures were optimized by the MOPAC/AM1 method,[8] after which the INDO/S method[9] was used for spectroscopic calculations. The calculated absorption wavelengths and the transition character of the first absorption bands are collected in Table 2. The calculated absorption wavelengths and the oscillator strength values are relatively well compatible with the observed spectra in benzene, although the calculated absorption spectra are blue-shifted. This deviation of the INDO/S calculations, giving high

Table 1. Absorption and fluorescence spectroscopic data for **1** and **2** in various solvents.

Compound	Solvent	Absorption (obs.)[a] λ_{max} [nm] (ε_{max} [dm^3 mol^{-1} cm^{-1}])	Fluorescence (obsd.)[b] λ_{em} [nm]	Φ[c]	SS[d] $\Delta\lambda_{max}$ [nm]
1	cyclohexane	371 (1730), 317 (17400)	480	0.12	109
	benzene	391 (1600), 321 (17300)	540	0.056	149
	1,4-dioxane	384 (1480), 320 (16200)	547	0.045	163
	tetrahydrofuran	385 (1230), 320 (17500)	555	0.020	170
	chloroform	398 (1260), 324 (17100)	566	0.006	168
	acetonitrile	388 (1310), 322 (16700)	–[e]	–[e]	–[e]
	ethanol (95%)	391 (1390), 320 (17700)	–[e]	–[e]	–[e]
2a	benzene	383 (1660), 321 (17700)	536	0.118	153
2b	cyclohexane	378 (1840), 317 (19000)	481	0.20	103
	benzene	392 (1700), 323 (18400)	537	0.11	145
	1,4-dioxane	388 (1660), 321 (18300)	568	0.077	180
	tetrahydrofuran	388 (1600), 321 (17800)	572	0.037	184
	chloroform	396 (1480), 325 (17200)	585	0.008	189
	acetonitrile	388 (1460), 323 (17200)	–[e]	–[e]	–[e]
	ethanol (95%)	392 (1440), 321 (19300)	–[e]	–[e]	–[e]
2c	benzene	391 (1620), 321 (17200)	537	0.112	146
2e	benzene	389 (1700), 322 (17900)	525	0.10	136
2f	benzene	383 (1900), 321 (19100)	535	0.111	152
2g	benzene	380 (2320), 324 (18500)	522	0.198	142

[a] 5.0×10^{-5} M. [b] 1.0×10^{-6} M. [c] Φ values were determined using 9,10-diphenylanthracene (Φ = 0.67, λex = 357 nm) in benzene as the standard. [d] Stokes shift value. [e] Too weak to be measured.

transition energies compared with the experimental values, has been observed generally.[10] The calculations show that the longest excitation bands for **1** and **2** are mainly attributable to the transitions from the HOMOs to the LUMOs, where the HOMOs were mostly localized on the 3-dibutylaminobenzofurano moieties and the LUMOs were mostly localized on the naphthoquinol moieties (Figure 1). The values of the dipole moments in the ground states are 2.79 for **1** and 3.11–3.38 for **2**. The differences between the dipole moments ($\Delta\mu$) of the first excited (HOMO→LUMO) and the ground states are 12.37 for **1** and 11.54–12.04 for **2**. The changes in the calculated electron density accompanying the first electron excitation are shown in Figure 2, which shows a strong migration of intramolecular charge-transfer character in **1** and **2**. On the other hand, the differences between the dipole moments ($\Delta\mu$) of the second excited (HOMO→LUMO + 1) and the ground states are 6.83 for **1** and 5.65–6.71 for **2**. These calculations indicate that compounds **1** and **2** have similarly large dipole moments in their excited states, which explains very well the experimental observations that the compounds showed large bathochromic shifts of their fluorescence maxima in polar solvents and that the Stokes shift values for compounds **1** and **2** in ethanol are much larger than those in benzene. The calculated data for **2** are quite similar to those for **1**, which is also in good agreement with the observation that these compounds exhibit similar Stokes shift values.

Table 2. Calculated absorption wavelengths (λ_{max}) and difference in dipole moments ($\Delta\mu$) for **1** and **2**.

	μ (D)[a]	Absorption (calcd.)			
		λ_{max} [nm]	f[b]	CI component[c]	$\Delta\mu$ [D][d]
1	2.79	356	0.12	HOMO→LUMO (87%)	12.37
		298	0.70	HOMO→LUMO + 1 (66%)	6.83
2a	3.16	352	0.11	HOMO→LUMO (87%)	11.57
		296	0.66	HOMO→LUMO + 1 (65%)	5.67
2b	3.19	355	0.11	HOMO→LUMO (87%)	12.04
		298	0.69	HOMO→LUMO + 1 (67%)	6.44
2c	3.11	352	0.11	HOMO→LUMO (87%)	11.54
		296	0.67	HOMO→LUMO + 1 (66%)	5.76
2e	3.14	352	0.11	HOMO→LUMO (87%)	11.57
		296	0.66	HOMO→LUMO + 1 (65%)	5.65
2f	3.22	352	0.12	HOMO→LUMO (87%)	11.54
		296	0.67	HOMO→LUMO + 1 (66%)	5.80
2g	3.38	357	0.13	HOMO→LUMO (88%)	11.56
		299	0.64	HOMO→LUMO + 1 (70%)	6.71

[a] The values of the dipole moment in the ground state. [b] Oscillator strength. [c] The transition is shown by an arrow from one orbital to another, followed by its percentage CI (configuration interaction) component. [d] The values of the difference in the dipole moment between the excited and the ground states.

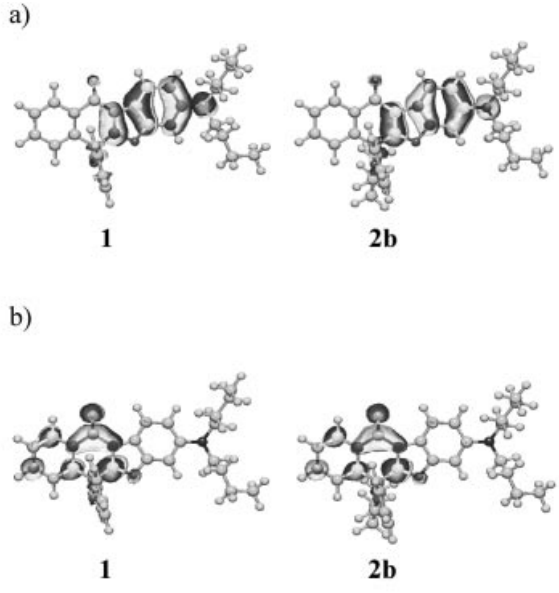

Figure 1. a) HOMOs and b) LUMOs for **1** and **2b**. The black and white lobes denote the negative and positive signs of the coefficients of the molecular orbital. The size of each lobe is proportional to the MO coefficient.

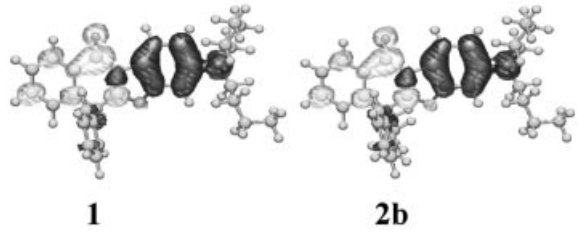

Figure 2. Calculated electron density changes accompanying the first electronic excitation of **1** and **2b**. The black and white lobes signify decreases and increases in electron density accompanying the electronic transition. Their areas indicate the magnitude of the electron density change.

Spectroscopic Properties of 1 and Alkoxy Derivatives 2 in the Solid State

Of particular interest are the photophysical properties of crystals of **1** and of the alkoxy derivatives **2**. Crystals of **1**, **2a**, **2b**, **2c**, **2f** and **2g** were obtained by recrystallization from ethanol solutions. Compound **2d**, however, was obtained in an amorphous state on recrystallization from various solutions (ethanol, *n*-hexane, acetonitrile, dichloromethane, benzene and acetone solutions). Crystals of **2e**, on the other hand, were obtained by dissolving in a minimum quantity of dichloromethane and reprecipitating with *n*-hexane. Figure 3 and Table 3 show the spectroscopic properties of the crystals of the fluorophores **1**, **2a**, **2b**, **2c**, **2e**, **2f** and **2g**. Many remarkable differences can be seen if the absorption and fluorescence spectra in the crystalline state are compared to those in solution. The longest wavelength of the excitation maximum of **1** is located at around 504 nm, which is red-shifted by 113 nm in comparison with the value of the absorption maximum in benzene. The fluorescence maximum of **1** is located at around 569 nm, which is red-shifted by 29 nm in comparison with the fluorescence maximum in benzene. On the other hand, the longest excitation maxima of the crystals of compounds **2** are located at around 444–503 nm, red-shifted by 55–128 nm in com-

parison with the longest absorption maxima of those in benzene, while the solid-state fluorescence maxima of compounds **2** are located at around 525–561 nm, red-shifted by 1–39 nm in comparison with the fluorescence maxima in benzene. The red shift values of **2** – except for **2g** – between solution and the solid state are smaller than that of **1**. Furthermore, large differences in fluorescence intensity between compounds **1** and **2** are clear. In the crystalline state, compounds **2** exhibit stronger fluorescence bands than compound **1**, which is quite different from the corresponding behaviour in solution: the fluorescence quantum yields of **1** and **2** in the crystalline state are in the order **2e** (Φ = 0.51) > **2b** (Φ = 0.26) > **2c** (Φ = 0.11) > **2a** (Φ = 0.04) ≈ **1** (Φ = 0.04). The fluorophores **2b** and **2e** exhibited much stronger fluorescence in the solid state than in solution. It has been reported that nonradiative decay is accelerated by free rotation of substituents in solution,[4d] and since the rotation of the alkoxy substituents is restricted in the solid state, the fluorescence quantum yields are higher in the solid states than in solution. The difference in the fluorescence quantum yields among various alkoxy derivatives in the crystalline state is discussed on the bases of the X-ray crystal structures in the next section.

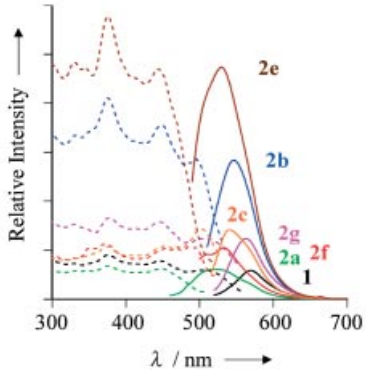

Figure 3. Solid-state excitation (dotted line) and emission (solid line) spectra of the crystals of **1**, **2a**, **2b**, **2c**, **2e**, **2f** and **2g**; **1**: λ_{ex} = 504 nm, λ_{em} = 569 nm; **2a**: λ_{ex} = 448 nm, λ_{em} = 525 nm; **2b**: λ_{ex} = 495 nm, λ_{em} = 547 nm; **2c**: λ_{ex} = 503 nm, λ_{em} = 540 nm; **2e**: λ_{ex} = 444 nm, λ_{em} = 527 nm; **2f**: λ_{ex} = 491 nm, λ_{em} = 536 nm; **2g**: λ_{ex} = 508 nm, λ_{em} = 561 nm.

Table 3. Spectroscopic properties of **1** and **2** in the crystalline state.

Compound	λ_{max}^{ex} [nm]	λ_{max}^{fl} [nm]	Φ [a]
1	504	569	0.04
2a	448	525	0.03
2b	495	547	0.26
2c	503	540	0.11
2e	444	527	0.51
2g	508	561	0.11

[a] The solid-state fluorescence quantum yields (Φ) were determined by using a calibrated integrating sphere system (λ_{ex} = 325 nm).

X-ray Crystal Structures of 1, 2a, 2b, 2c and 2f

To understand the dramatic substituent effects on the solid-state photophysical properties, the X-ray crystal structures of compound **1** and of its alkoxy derivatives **2a**, **2b**, **2c** and **2f** have been determined and are shown in Figures 4, 5, 6, 7, and 8, respectively, while the crystal systems of **1** and the alkoxy derivatives **2** are summarized in Table 4. The packing structures show that the molecules of **1**, **2a**, **2b**, **2c** and **2f** are arranged in a "bricks in a wall" fashion.

The packing structures demonstrate that the crystal of **1** is made up of a centrosymmetric dimer unit composed of a pair of quinol enantiomers bound cofacially by intermolecular hydrogen bonds between the hydroxy group and the carbonyl group on both sides of the dimer unit. The OH···O hydrogen bond angle is 179(3)° and the O···O distance is 2.811(2) Å. The two hydrogen bonds hold the enantiomers in close proximity, leading to close π–π overlapping. As shown in Figure 4 (c), there are 8 (= 4×2) short interatomic π–π contacts for **1**. The π–overlaps were observed between the naphthoquinol moieties. The interplanar distances between the naphtho[2,3-*b*]benzofuran planes are ca. 3.57 Å, which suggests strong π–π interactions between the fluorophores.

In the case of the alkoxy derivatives, on the other hand, there are no intermolecular hydrogen bonds between the enantiomers. The phenyl group is twisted out of the plane of the naphtho[2,3-*b*]benzofuran moiety by ca. 90° and the alkoxy chain is also almost perpendicularly extended to the π–plane. In the crystal of **2a**, continuous π-stacking of identical enantiomers (*R* or *S*) is produced in independent columns in which π-overlapping can be observed between the naphtho moieties and the 9-dibutylaminobenzo moieties of the adjacent identical enantiomers (Figure 5). The interplanar distances between the naphtho[2,3-*b*]benzofuran planes are ca. 3.42 Å. There are six short interatomic π–π contacts of less than 3.6 Å in a pair of enantiomers, which suggests π–π interactions between the fluorophores.

In the case of **2b**, there are no short nonbonded interatomic π–π contacts of less than 3.60 Å, as can be seen in Figure 6. The phenyl group is twisted out of the plane of the naphtho[2,3-*b*]benzofuran moiety by 90.24° and the butoxy chain is also almost perpendicularly extended to the quinol plane. The shortest distance for non-bonded overlapping atoms is 3.81(3) Å [for C(11)*···C(12) and C(11)···C(12)*], which suggests a considerable reduction in the intermolecular π–π interactions between neighbouring fluorophores.

The packing structures of **2c** and **2f** resemble one another very closely, as shown in Figure 7 and Figure 8. There are three short interatomic π–π contacts of less than 3.6 Å in a pair of identical enantiomers. The inclination between the naphtho[2,3-*b*]benzofuran planes in the pair of identical enantiomers are 27° for **2c** and 28° for **2f**. These results demonstrated that alkoxylation of fluorophores can effectively prevent the intermolecular π–π interaction[3b,5,4,11–14] and intermolecular hydrogen bonding[2b,15] between fluorophores in the molecular aggregation state and thus cause a dramatic enhancement in the solid-state fluorescence.

From the stereostructures of **2a**, **2b**, **2c** and **2f** we noticed that the chain lengths of the alkoxy substituents affected the crystal structures (Figure 9). Consequently, the degree

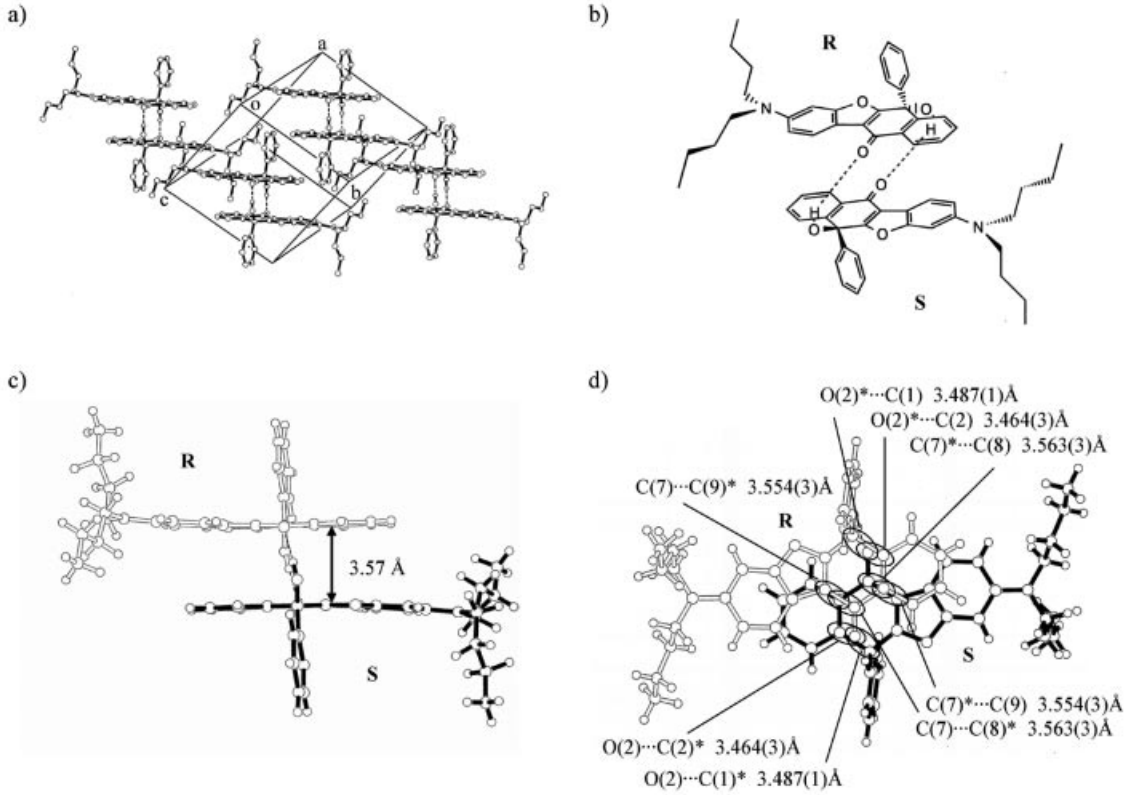

Figure 4. Crystal packing and hydrogen bonding pattern of **1**; a) a stereoview of the molecular packing structure, b) a schematic structure, c) a side view, and d) a top view of the pairs of fluorophores.

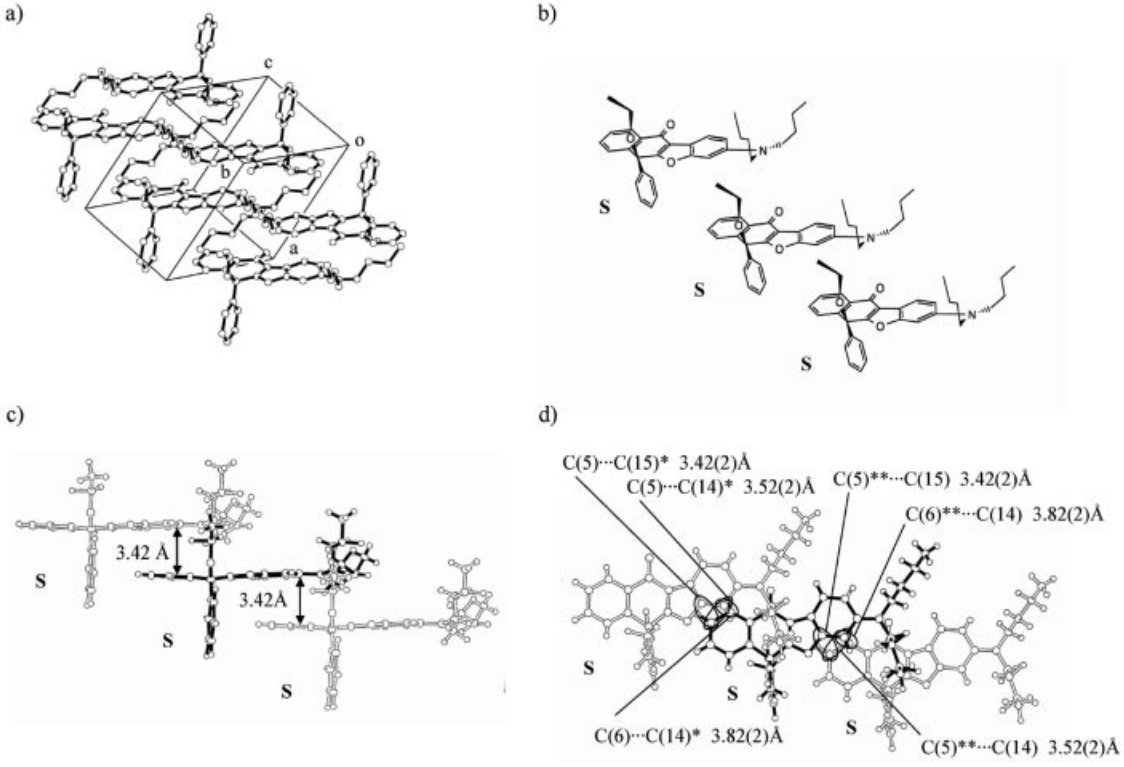

Figure 5. Crystal packing of **2a**; a) a stereoview of the molecular packing structure, b) a schematic structure, c) a side view, and d) a top view of the pairs of fluorophores.

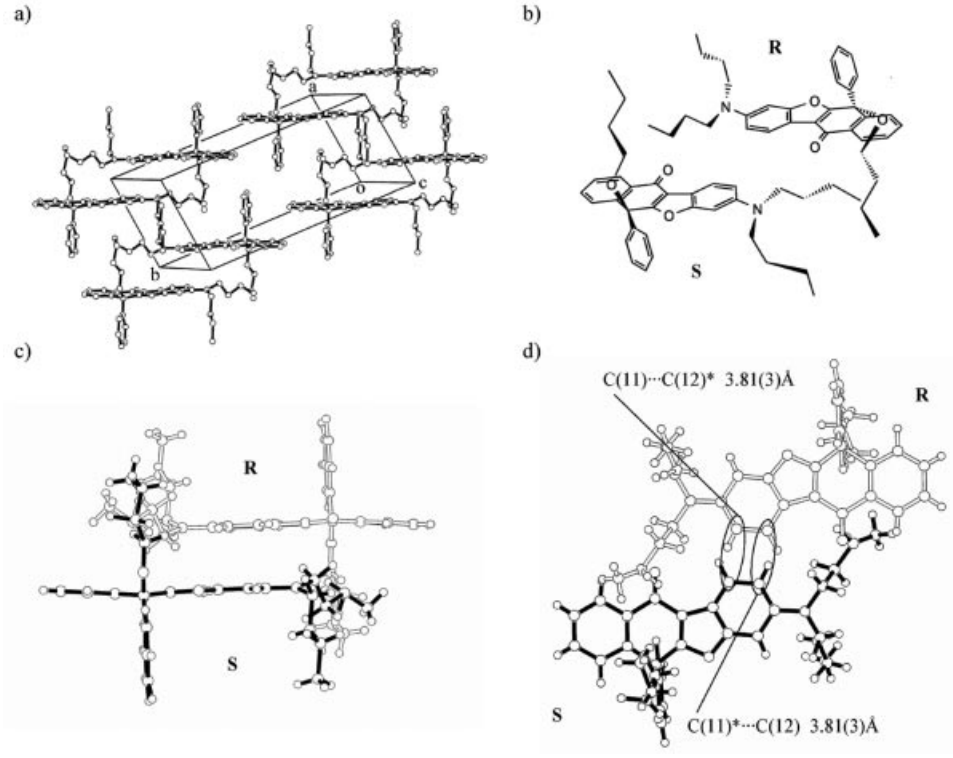

Figure 6. Crystal packing of **2b** a) a stereoview of the molecular packing structure, b) a schematic structure, c) a side view, and d) a top view of the pairs of fluorophores.

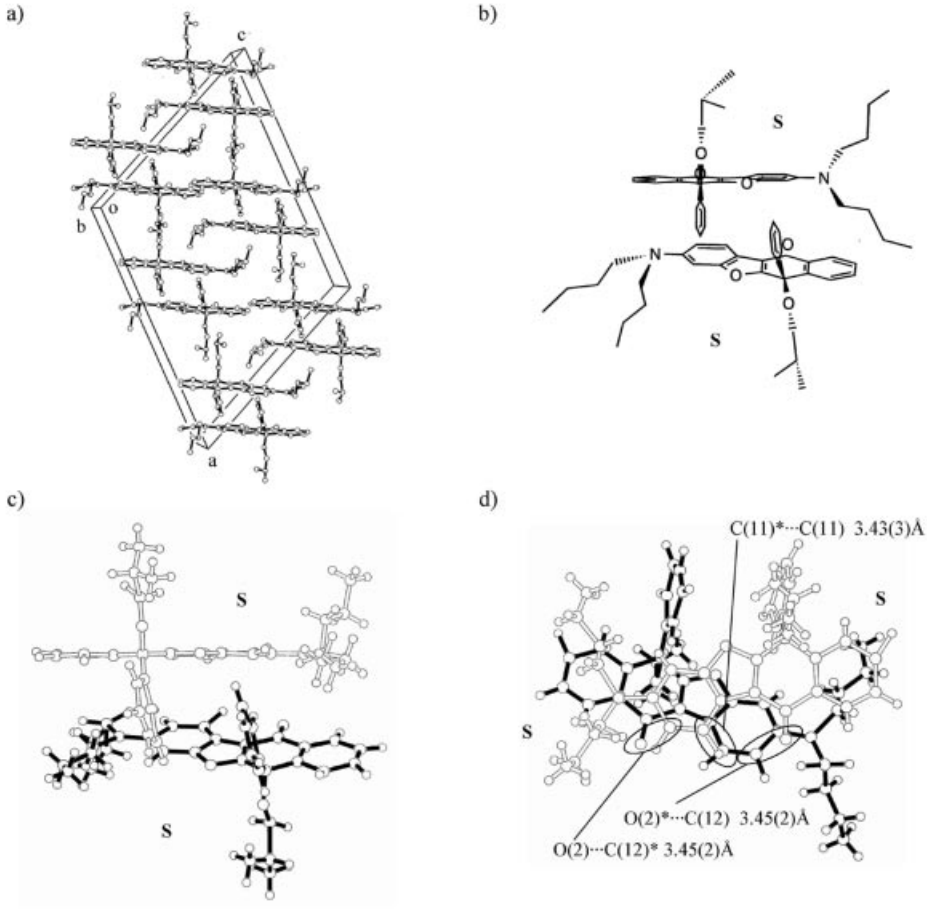

Figure 7. Crystal packing of **2c**; a) a stereoview of the molecular packing structure, b) a schematic structure, c) a side view, and d) a top view of the pairs of fluorophores.

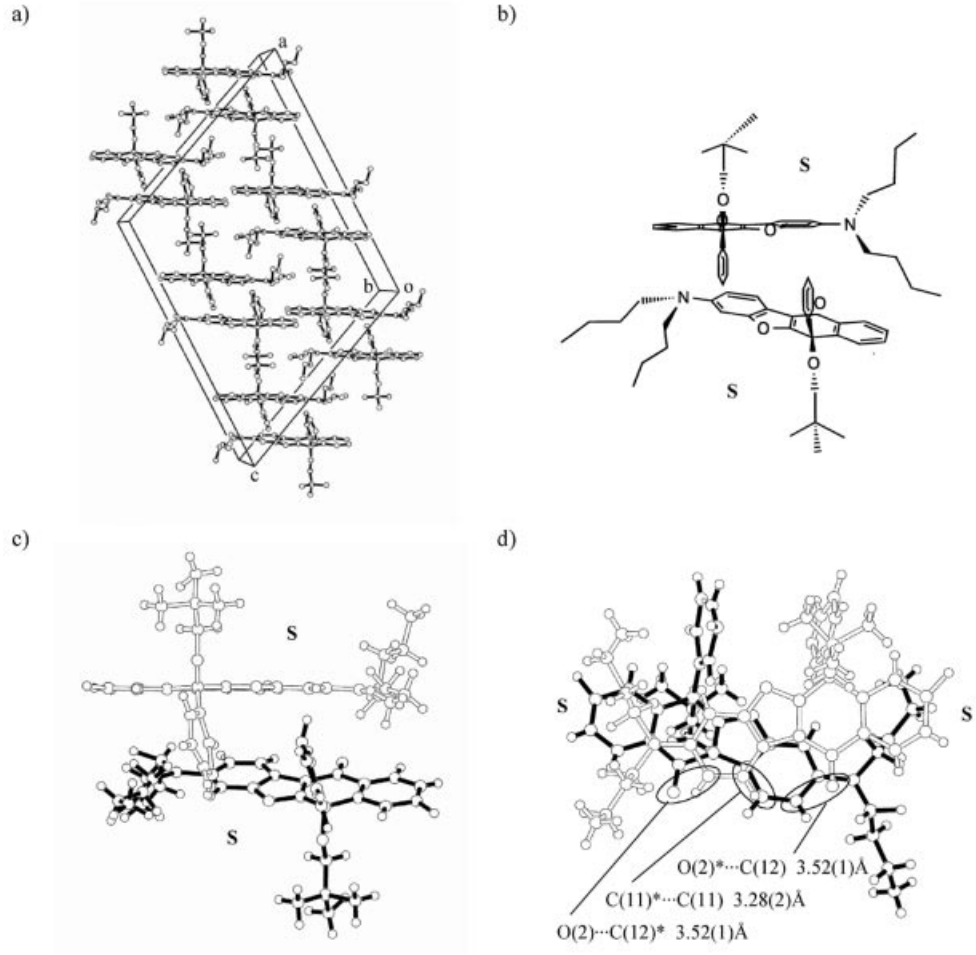

Figure 8. Crystal packing of **2f**; a) a stereoview of the molecular packing structure, b) a schematic structure, c) a side view, and d) a top view of the pairs of fluorophores.

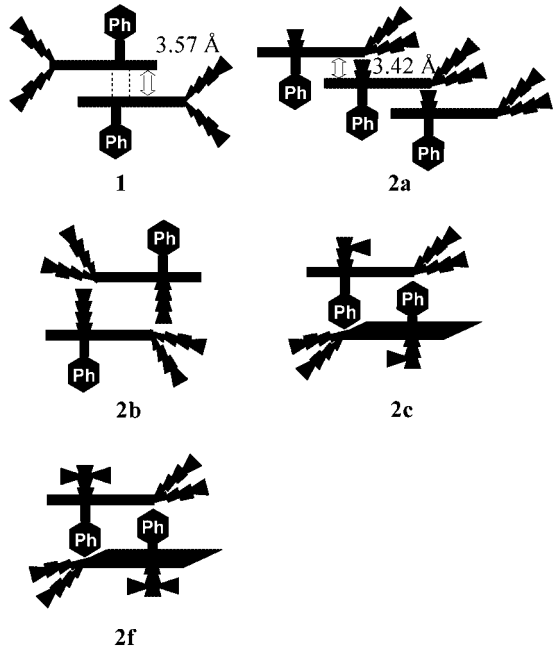

Figure 9. Schematic representation of the effects of the substituents on the interplanar distances between a pair of fluorophores for **1**, **2a**, **2b**, **2c** and **2f**.

of reduction in the intermolecular π–π interactions and the interplanar distances between neighbouring fluorophores are closely related to the lengths of the alkyl chains in the alkoxy substituents. In the case of **2a**, continuous π–stacking of identical enantiomers (either *R* or *S*) in independent columns was found, because the short chain of the ethoxy substituent cannot efficiently prevent short π–π contacts between the fluorophores in the molecular aggregation state. In the cases of **2c** and **2f**, some short interatomic π–π contacts of less than 3.6 Å in a pair of equal enantiomers were still observable because the isobutoxy and neopentoxy substituents are not sufficient to prevent short π–π contacts between the fluorophores. In contrast, in the case of **2b**, there are no short interatomic π–π contacts of less than 3.60 Å. This result indicates that the butoxy substituent can efficiently prevent short π–π contacts between the fluorophores and lead to much stronger solid-state fluorescence emission. As shown above, a good correlation between the solid-state fluorescence intensity and the molecular stacking structure was observed. In addition, it was demonstrated that the pentoxy substituent of **2e** is effective for the appearance of strong solid-state fluorescence, although no high-quality single crystal of **2e** could be obtained. On the other hand, Ooyama et al. reported that for benzofuro[2,3-*c*]oxa-

zolo[4,5-*a*]carbazole-type fluorescent dyes the introduction of sterically hindered substituents onto a carbazole ring situated on the centre of a chromophore skeleton can efficiently prevent short π–π contacts between the fluorophores in molecular aggregation states and cause a dramatic solid-state fluorescence enhancement.[16] In the case of the compounds **2**, it was demonstrated that the introduction of bulky 6,6-disubstituents (such as a phenyl group and a long alkoxy group) in non-conjugated linkage to the centre of the chromophore skeleton can have a large effect for the improvement of the solid-state fluorescence.

Conclusions

We have synthesized heterocyclic 6-alkoxy-3-dibutylamino-6-phenylnaphtho[2,3-*b*]benzofuran-11(6*H*)-one fluorophores each containing a phenyl group and one of various alkoxy substituents linked in non-conjugated fashion to the chromophore skeleton at the 6-position and have evaluated their absorption and fluorescence properties in solution and in the solid state. It was confirmed that the introduction of long-chain alkoxy substituents in non-conjugated linkage to the centre of the chromophore skeleton can efficiently prevent short π–π contacts between the fluorophores in molecular aggregation states and cause dramatic solid-state fluorescence enhancement.

Experimental Section

General: Melting points were measured with a Yanaco MP-500D micro melting point apparatus. IR spectra were recorded on a JASCO FT/IR-5300 spectrophotometer with samples in KBr pellet form. Absorption spectra were observed with a JASCO U-best30 spectrophotometer, and fluorescence spectra were measured with a JASCO FP-777 spectrophotometer. Single-crystal X-ray diffraction was performed with a Rigaku AFC7S diffractometer. For the measurement of the solid-state fluorescence excitation and emission spectra of the crystals, a JASCO FP-777 spectrometer with a JASCO FP-1060 attachment was used. The fluorescence quantum yields (Φ) in solution were determined with 9,10-diphenylanthracene (Φ = 0.67, λ_{ex} = 357 nm)[17] in benzene as the standard. The solid-state fluorescence quantum yields (Φ) were determined by use of a calibrated integrating sphere system (λ_{ex} = 325 nm). Elemental analyses were recorded on a Perkin–Elmer 2400 II CHN analyzer. ^{1}H NMR spectra were recorded on a JNM-LA-400 (400 MHz) FT NMR spectrometer with tetramethylsilane (TMS) as an internal standard. Column chromatography was performed on silica gel (KANTO CHEMICAL, 60 N, spherical, neutral). Semiempirical molecular orbital (MO) calculations were performed with a FUJITSU FMV-ME4/657 by use of the WinMOPAC Ver. 3 package (Fujitsu, Chiba, Japan).

General Synthetic Procedure for 6-Alkoxy-3-(dibutylamino)-6-phenylnaphtho[2,3-*b*]benzofuran-11(6*H*)-ones 2a–2g by Dehydroxybutoxylation of 1: Compound **1** (0.3 g) was dissolved in a solution of BF_3·OEt_2 (47%, 17 mL) and the system was stirred for 15 min at room temperature. The reaction mixture was poured into water and the resulting precipitate was filtered and dried to afford a cationic salt as a dark green powder (0.37 g, 93% yield). The cationic salt (0.3 g) was dissolved in the appropriate alcohol and the system was stirred for 30 min at 60 °C. The reaction mixture was neutralized with aq. Na_2CO_3 and extracted with $CHCl_3$. The organic extract was washed with water and the solvents were evaporated. The residue was chromatographed on silica gel (CH_2Cl_2 as eluent) and was further purified by recrystallization from a mixture of CH_2Cl_2/*n*-hexane to give **2a**–**2g** as yellow and orangish yellow crystals.

A**3-(Dibutylamino)-6-ethoxy-6-phenylnaphtho[2,3-*b*]benzofuran-11(6*H*)-one (2a):** Yield 79%; m.p. 160–163 °C. ^{1}H NMR (400 MHz, [D_3]chloroform, TMS): δ = 0.93 (t, 6 H), 1.18 (t, 3 H), 1.33–1.62 (m, 8 H), 3.10–3.40 (m, 6 H), 6.76 (d, J = 2.2 Hz, 1 H), 6.86 (dd, J = 2.2 and 8.8 Hz, 1 H), 7.22–7.66 (m, 8 H), 7.92 (d, J = 8.7 Hz, 1 H), 8.25 (dd, J = 1.0 and 7.6 Hz, 1 H) ppm. IR (KBr): $\tilde{\nu}$ = 1667 cm^{-1}. $C_{32}H_{35}NO_3$ (481.63): calcd. C 79.80, H 7.32, N 2.91; found C 79.74, H 7.54, N 3.03.

6-Butoxy-3-(dibutylamino)-6-phenylnaphtho[2,3-*b*]benzofuran-11(6*H*)-one (2b): Yield 86%; m.p. 115–117 °C. ^{1}H NMR (400 MHz, [D_3]chloroform, TMS): δ = 0.84 (t, 3 H), 0.95 (t, 6 H), 1.26–1.61 (m, 12 H), 3.04–3.21 (m, 2 H), 3.29 (t, 4 H), 6.69 (d, J = 2.2 Hz, 1 H), 6.75 (dd, J = 2.2 and 8.8 Hz, 1 H), 7.21–7.54 (m, 8 H), 8.01 (d, J = 8.5 Hz, 1 H), 8.33 (dd, J = 1.2 and 7.8 Hz, 1 H) ppm. IR (KBr): $\tilde{\nu}$ = 1660 cm^{-1}. $C_{34}H_{39}NO_3$ (509.68): calcd. C 80.12, H 7.71, N 2.75; found C 80.19, H 7.92, N 2.89.

3-(Dibutylamino)-6-isobutoxy-6-phenylnaphtho[2,3-*b*]benzofuran-11(6*H*)-one (2c): Yield 68%; m.p. 123–126 °C. ^{1}H NMR (400 MHz, [D_6]acetone, TMS): δ = 0.88–0.97 (m, 12 H), 1.26–1.61 (m, 8 H), 1.90–1.93 (m, 1 H), 2.78–2.99 (m, 2 H), 3.29 (t, 4 H), 6.70–6.77 (m, 2 H), 7.22–7.55 (m, 8 H), 8.02 (d, J = 8.5 Hz, 1 H), 8.33 (d, J = 7.8 Hz, 1 H) ppm. IR (KBr): $\tilde{\nu}$ = 1662 cm^{-1}. $C_{34}H_{39}NO_3$ (509.68): calcd. C 80.12, H 7.71, N 2.75; found C 80.22, H 7.91, N 2.88.

6-*tert*-Butoxy-3-(dibutylamino)-6-phenylnaphtho[2,3-*b*]benzofuran-11(6*H*)-one (2d): Yield 62%; m.p. 42–45 °C. ^{1}H NMR (400 MHz, [D_6]acetone, TMS): δ = 0.58–0.93 (m, 15 H), 1.36–1.60 (m, 8 H), 3.32 (t, 4 H), 6.76–6.86 (m, 2 H), 7.25–7.59 (m, 8 H), 7.90–7.93 (m, 1 H), 8.25–8.28 (m, 1 H) ppm. IR (KBr): $\tilde{\nu}$ = 1658 cm^{-1}. $C_{34}H_{39}NO_3$ (509.68): calcd. C 80.12, H 7.71, N 2.75; found C 80.35, H 8.05, N 2.79.

3-(Dibutylamino)-6-pentoxy-6-phenylnaphtho[2,3-*b*]benzofuran-11(6*H*)-one (2e): Yield 54%; m.p. 107–109 °C. ^{1}H NMR (400 MHz, [D_3]chloroform, TMS): δ = 0.85 (t, 3 H), 0.95 (t, 6 H), 1.26–1.61 (m, 14 H), 3.04–3.20 (m, 2 H), 3.29 (t, 4 H), 6.69 (d, J = 2.2 Hz, 1 H), 6.74 (dd, J = 2.2 and 8.8 Hz, 1 H), 7.22–7.54 (m, 8 H), 8.01 (d, J = 8.8 Hz, 1 H), 8.32 (dd, J = 1.2 and 7.8 Hz, 1 H) ppm. IR (KBr): $\tilde{\nu}$ = 1665 cm^{-1}. $C_{35}H_{41}NO_3$ (523.70): calcd. C 80.27, H 7.89, N 2.67; found C 80.33, H 7.62, N 2.81.

3-(Dibutylamino)-6-neopentoxy-6-phenylnaphtho[2,3-*b*]benzofuran-11(6*H*)-one (2f): Yield 55%; m.p. 123–126 °C. ^{1}H NMR (400 MHz, [D_3]chloroform, TMS): δ = 0.92–0.96 (m, 15 H), 1.32–1.38 (m, 4 H), 1.53–1.59 (m, 4 H), 2.77 (m, 2 H), 3.26–3.31 (m, 4 H), 6.69–6.77 (m, 2 H), 7.2–7.29 (m, 4 H), 7.43–7.54 (m, 4 H), 8.02 (d, J = 8.78 Hz, 1 H), 8.32 (d, J = 6.3 Hz, 1 H) ppm. IR (KBr): $\tilde{\nu}$ = 1662 cm^{-1}. $C_{35}H_{41}NO_3$ (523.70): calcd. C 80.27, H 7.89, N 2.67; found C 80.09, H 8.01, N 2.72.

3-(Dibutylamino)-6-phenoxy-6-phenylnaphtho[2,3-*b*]benzofuran-11(6*H*)-one (2g): Yield 71%; m.p. 226–228 °C. ^{1}H NMR (400 MHz, [D_6]acetone, TMS): δ = 0.92 (t, 6 H), 1.3–1.6 (m, 8 H), 3.36 (t, 4 H), 6.74–6.78 (m, 2 H), 7.03–7.35 (m, 10 H), 7.41 (dd, J = 1.24 and 7.80 Hz, 1 H), 7.51 (dd, J = 1.24 and 7.32 Hz, 1 H), 7.58 (dd, J = 1.48 and 7.32 Hz, 1 H) 7.91 (d, J = 8.76 Hz, 1 H), 8.32 (dd, J = 1.48 and 7.56 Hz, 1 H) ppm. IR (KBr): $\tilde{\nu}$ = 1637 cm^{-1}. $C_{36}H_{35}NO_3$ (529.67): calcd. C 81.63, H 6.66, N 2.64; found C 81.70, H 6.60, N 2.70.

Table 4. Crystal data and structure refinement parameters for compounds **1** and **2**.

Compound	**1**	**2a**	**2b**	**2c**	**2f**
Molecular formula	$C_{30}H_{31}NO_3$	$C_{32}H_{35}NO_3$	$C_{34}H_{39}NO_3$	$C_{34}H_{39}NO_3$	$C_{35}H_{41}NO_3$
Formula weight	453.58	481.63	509.69	509.69	523.71
Crystal size[nm]	0.55 × 0.10 × 0.70	0.20 × 0.05 × 0.20	0.30 × 0.10 × 0.40	0.60 × 0.30 × 0.25	0.25 × 0.30 × 0.40
Refine (2θ range [°])[a]	25 (27.2–29.6)	9 (6.6–17.5)	25 (22.4–24.9)	25 (20.1–25.4)	25 (22.1–24.0)
Crystal system	triclinic	triclinic	triclinic	monoclinic	monoclinic
Space group	$P\bar{1}$	$P\bar{1}$	$P\bar{1}$	$C2/c$	$C2/c$
a [Å]	11.738(2)	10.131(6)	9.061(1)	26.377(4)	26.429(7)
b [Å]	12.244(2)	15.851(6)	20.227(2)	11.253(4)	11.321(1)
c [Å]	10.879(2)	8.247(5)	8.751(1)	21.601(4)	21.860(8)
α [°]	90.69(2)	93.96(5)	101.52(1)		
β [°]	116.39(1)	91.22(6)	114.30(1)	114.79(1)	113.10(2)
γ [°]	64.73(1)	84.87(4)	87.75(1)		
V [Å^3]	1235.8(10)	1315(1)	1430.6(4)	5821(2)	6016(2)
Z	2	2	2	8	8
$\rho_{calcd.}$ [g cm^{-3}]	1.219	1.216	1.183	1.163	1.156
$F(000)$	484.00	516.00	548.0	2192.0	2256.0
$\mu(Mo_{K\alpha})$ [cm^{-1}]	0.78	0.77	0.74	0.73	0.72
T [K]	296.2	296.2	296.2	296.2	296.2
Scan mode	ω–2θ	ω–2θ	ω–2θ	ω–2θ	ω–2θ
Scan rate [ωmin^{-1}]	4.0[b]	4.0[b]	4.0[b]	4.0[b]	4.0[b]
Scan width [°]	1.68 + 0.30 tanθ	1.37 + 0.30 tanθ	1.10 + 0.30 tanθ	1.78 + 0.30 tanθ	0.94 + 0.30 tanθ
2θ max. [°]	50.0	50.0	50.0	50.0	50.0
hkl range	–13/0, –14/13, –11/12	0/12, –18/18, –9/9	0/10, –24/24, 10/9	0/31, 0/13, –25/23	0/28, –12/12, –23/21
Reflections measured	4577	4914	5385	5243	7824
Unique reflections	4345	4629	5036	5122	4916
Reflections obsd. with $I_0 > 2\sigma I_0$	2631	1336	2304	1606	2060
R_{int}	0.015	0.104	0.045	0.062	0.066
Number of parameters	432	398	432	374	389
R	0.0406	0.0856	0.0803	0.1287	0.1027
Rw	0.0986	0.1613	0.1700	0.2552	0.2162
w	$(\sigma^2F^2)^{-1}$	$(\sigma^2F^2)^{-1}$	$(\sigma^2F^2)^{-1}$	$(\sigma^2F^2)^{-1}$	$(\sigma^2F^2)^{-1}$
S	1.19	1.04	1.33	1.78	1.60
Max. shift/error in final cycle	0.01	0.01	0.01	0.00	0.01
Max. peak in final diff. map [e Å^{-3}]	0.34	0.43	0.41	0.78	0.45
min. peak in final diff. map [e Å^{-3}]	–0.28	–0.46	–0.32	–0.66	–0.38

[a] Number of reflections used for unit cell determination. [b] Up to five scans.

X-ray Crystallographic Studies: The reflection data were collected at 23 ± 1 °C on a Rigaku AFC7S four-circle diffractometer by the 2θ–ω scan technique and with use of graphite-monochromated Mo-K_α (λ = 0.71069 Å) radiation at 50 kV and 30 mA. In all cases the data were corrected for Lorentz and polarization effects. A correction for secondary extinction was applied. The reflection intensities were monitored by three standard reflections for every 150 reflections. An empirical absorption correction based on azimuthal scans of several reflections was applied. All calculations were performed using the teXsan[18] crystallographic software package (Molecular Structure Corporation).

CCDC-172461 (for **1**), -635416 (for **2a**), -172462 (for **2b**), -635417 (for **2c**) and -635418 (for **2f**) contain the supplementary crystallographic data for this paper. These data can be obtained free of charge from The Cambridge Crystallographic Data Centre via www.ccdc.cam.au.uk/data_request/cif. See also Table 4.

Compound 1: Crystals of **1** were recrystallized from ethanol to give orange, air-stable prisms. The transmission factors ranged from 0.98 to 1.00. The crystal structure was solved by direct methods using SIR 88.[19] The structures were expanded by Fourier techniques.[20] The non-hydrogen atoms were refined anisotropically. Some hydrogen atoms were refined isotropically, the rest were fixed geometrically and not refined.

Compound 2a: Crystals of **2a** were recrystallized from ethanol as yellow, air-stable prisms. The transmission factors ranged from 0.93 to 1.00. The crystal structure was solved by direct methods using SAPI 91.[21] The structures were expanded by Fourier techniques.[20] The non-hydrogen atoms were refined anisotropically. Some hydrogen atoms were refined isotropically, the rest were fixed geometrically and not refined.

Compound 2b: Crystals of **2b** were recrystallized from ethanol as yellow, air-stable prisms. The transmission factors ranged from 0.97 to 1.00. The crystal structure was solved by direct methods using SIR 92.[22] The structures were expanded by Fourier techniques.[20] The non-hydrogen atoms were refined anisotropically. Some hydrogen atoms were refined isotropically, the rest were fixed geometrically and not refined.

Compound 2c: Crystals of **2c** were recrystallized from ethanol as yellow, air-stable prisms. The transmission factors ranged from 0.95 to 1.00. The crystal structure was solved by direct methods using SIR 88.[19] The structures were expanded by Fourier techniques.[20] The non-hydrogen atoms were refined anisotropically. Some hydrogen atoms were refined isotropically, the rest were fixed geometrically and not refined.

Compound 2f: Crystals of **2f** were recrystallized from ethanol as yellow, air-stable prisms. The transmission factors ranged from 0.95

to 1.00. The crystal structure was solved by direct methods using SIR 88.[19] The structures were expanded by Fourier techniques.[16] The non-hydrogen atoms were refined anisotropically. Some hydrogen atoms were refined isotropically, the rest were fixed geometrically and not refined.

Computational Methods: All calculations were performed on a FUJITSU FMV-ME4/657. The semiempirical calculations were carried out with the WinMOPAC Ver. 3 package (Fujitsu, Chiba, Japan). Geometry calculations in the ground state were carried out by the AM1 method.[8] All geometries were completely optimized (keyword PRECISE) by the eigenvector following routine (keyword EF). Experimental absorption spectra of the compounds were studied by the semiempirical method INDO/S (intermediate neglect of differential overlap/spectroscopic).[9] All INDO/S calculations were performed using single excitation full SCF/CI (self-consistent field/configuration interaction), which includes the configuration with one electron excited from any occupied orbital to any unoccupied orbital; 225 configurations were considered for the configuration interaction [keyword CI (15 15)].

Acknowledgments

This work was partially supported by a Grant-in-Aid for Science and Research from the Ministry of Education, Science, Sport and Culture of Japan (Grant 18350100), by a Science and Technology Incubation Program in Advanced Regions of the Japan Science and Technology Agency (JST), and by a Special Research Grant for Green Science from Kochi University.

[1] a) C. W. Tang, S. A. VansSlyke, *Appl. Phys. Lett.* **1987**, *51*, 913–915; b) C. W. Tang, S. A. VansSlyke, C. H. Chen, *J. Appl. Phys.* **1989**, *65*, 3610–3616; c) J. Schi, C. W. Tang, *Appl. Phys. Lett.* **1997**, *70*, 1665–1667; d) A. Kraft, A. C. Grimsdale, A. B. Holmes, *Angew. Chem.* **1998**, *110*, 416–443; *Angew. Chem. Int. Ed.* **1998**, *37*, 402–428; e) U. Mitschke, P. Bäuerle, *J. Mater. Chem.* **2000**, *10*, 1471–1507; f) K.-C. Wong, Y.-Y. Chien, R.-T. Chen, C.-F. Wang, Y.-T. Liu, H.-H. Chiang, P.-Y. Hsieh, C.-C. Wu, C. H. Chou, Y. O. Su, G.-H. Lee, S.-M. Peng, *J. Am. Chem. Soc.* **2002**, *124*, 11576–11577; g) C. J. Tonzola, M. M. Alam, W. K. Kaminsky, S. A. Jenekhe, *J. Am. Chem. Soc.* **2003**, *125*, 13548–13558; h) H.-C. Yeh, L.-H. Chan, W.-C. Wu, C.-T. Chen, *J. Mater. Chem.* **2004**, *14*, 1293–1298; i) C.-T. Chen, *Chem. Mater.* **2004**, *16*, 4389–4400; j) C.-L. Chiang, M.-F. Wu, D.-C. Dai, Y.-S. Wen, J.-K. Wang, C.-T. Chen, *Adv. Funct. Mater.* **2005**, *15*, 231–238; k) D. Berner, C. Klein, M. D. Nazeeruddin, F. de Angelis, M. Castellani, P. Bugnon, R. Scopelliti, L. Zuppiroli, M. Graetzel, *J. Mater. Chem.* **2006**, *16*, 4468–4474.

[2] a) Z.-S. Wang, F.-Y. Li, C.-H. Hang, L. Wang, M. Wei, L.-P. Jin, N.-Q. Li, *J. Phys. Chem. B* **2000**, *104*, 9676–9682; b) A. Ehret, L. Stuhl, M. T. Spitler, *J. Phys. Chem. B* **2001**, *105*, 9960–9965; c) K. Hara, T. Sato, R. Katoh, A. Furube, Y. Ohga, A. Shinpo, S. Suga, K. Sayama, H. Sugihara, H. Arakawa, *J. Phys. Chem. B* **2003**, *107*, 597–606; d) K. R. J. Thomas, J. T. Kin, Y.-C. Hsu, K.-C. Ho, *Chem. Commun.* **2005**, 4098–4100; e) D. P. Hagberg, T. Edvinsson, T. Marinado, G. Boschloo, A. Hagfeld, L. Sun, *Chem. Commun.* **2006**, 2245–2247; f) S.-L. Li, K.-J. Jiang, K.-F. Shao, L.-M. Yang, *Chem. Commun.* **2006**, 2792–2794.

[3] a) R. Davis, S. Abraham, N. P. Rath, S. Das, *New J. Chem.* **2004**, *28*, 1368–1372; b) E. Horiguchi, S. Matsumoto, K. Funabiki, M. Matsui, *Bull. Chem. Soc. Jpn.* **2005**, *78*, 1167–1173.

[4] a) Y. Ooyama, T. Nakamura, K. Yoshida, *New J. Chem.* **2005**, *29*, 447–456; b) Y. Ooyama, T. Okamoto, T. Yamaguchi, T. Suzuki, A. Hayashi, K. Yoshida, *Chem. Eur. J.* **2006**, 7827–7838; c) Y. Ooyama, S. Yoshikawa, S. Watanabe, K. Yoshida, *Org. Biomol. Chem.* **2006**, *4*, 3406–3409; d) Y. Ooyama, S. Yoshikawa, S. Watanabe, K. Yoshida, *Org. Biomol. Chem.* **2007**, *5*, 1260–1269.

[5] H.-C. Yeh, W.-C. Wu, Y.-S. Wen, D.-C. Dai, J.-K. Wang, C.-T. Chen, *J. Org. Chem.* **2004**, *69*, 6455–6462.

[6] K. Yoshida, Y. Ooyama, H. Miyazaki, S. Watanabe, *J. Chem. Soc. Perkin Trans. 2* **2002**, 700–707.

[7] S. Nakatsuji, H. Nakazumi, H. Fukuma, T. Yahiro, K. Nakashima, M. Iyoda, S. Akiyama, *J. Chem. Soc. Perkin Trans. 1* **1991**, 1881.

[8] M. J. S. Dewar, E. G. Zoebisch, E. F. Healy, J. J. P. Stewart, *J. Am. Chem. Soc.* **1985**, *107*, 3902–3909.

[9] a) J. E. Ridley, M. C. Zerner, *Theor. Chim. Acta* **1973**, *32*, 111–134; b) J. E. Ridley, M. C. Zerner, *Theor. Chim. Acta* **1976**, *42*, 223–236; c) A. D. Bacon, M. C. Zerner, *Theor. Chim. Acta* **1979**, *53*, 21–54.

[10] a) M. Adachi, Y. Murata, S. Nakamura, *J. Org. Chem.* **1993**, *58*, 5238–5244; b) W. M. F. Fabian, S. Schuppler, O. S. Wolfbeis, *J. Chem. Soc. Perkin Trans. 2* **1996**, 853–856.

[11] a) Z. Fei, N. Kocher, C. J. Mohrschladt, H. Ihmels, D. Stalke, *Angew. Chem.* **2003**, *115*, 807–811; *Angew. Chem. Int. Ed.* **2003**, *42*, 783–787; b) J. L. Scott, T. Yamada, K. Tanaka, *New J. Chem.* **2004**, *28*, 447–450.

[12] a) K. Yoshida, J. Yamazaki, Y. Tagashira, S. Watanabe, *Chem. Lett.* **1996**, 9–10; b) K. Yoshida, T. Tachikawa, J. Yamasaki, S. Watanabe, S. Tokita, *Chem. Lett.* **1996**, 1027–1028; c) K. Yoshida, H. Miyazaki, Y. Miura, Y. Ooyama, S. Watanabe, *Chem. Lett.* **1999**, 837–838; d) K. Yoshida, Y. Ooyama, S. Tanikawa, S. Watanabe, *Chem. Lett.* **2000**, 714–715; e) K. Yoshida, Y. Ooyama, S. Tanikawa, S. Watanabe, *J. Chem. Soc. Perkin Trans. 2* **2002**, 708–714; f) Y. Ooyama, K. Yoshida, *New J. Chem.* **2005**, *29*, 1204–1212.

[13] H. Langhals, T. Potrawa, H. Nöth, G. Linti, *Angew. Chem.* **1989**, *101*, 497–499; *Angew. Chem. Int. Ed. Engl.* **1989**, *28*, 478–480.

[14] A. Dreuw, J. Plötner, L. Lorenz, J. Wachtveitl, J. E. Djanhan, J. Brüning, T. Metz, M. Bolte, M. U. Schmidt, *Angew. Chem.* **2005**, *117*, 7961–7964; *Angew. Chem. Int. Ed.* **2005**, *44*, 7783–7786.

[15] K. Yoshida, K. Uwada, H. Kumaoka, L. Bu, S. Watanabe, *Chem. Lett.* **2001**, 808–809.

[16] Y. Ooyama, Y. Harima, *Chem. Lett.* **2006**, 902–903.

[17] C. A. Heller, R. A. Henry, B. A. McLaughlin, D. E. Bills, *J. Chem. Eng. Data.* **1974**, *19*, 214–219.

[18] *teXsan*: Crystal Structure Analysis Package, Molecular Structure Corporation **1985** and **1992**.

[19] M. C. Burla, M. Camalli, G. Cascaeano, C. Giacovazzo, G. Polidori, R. Spagna, D. Viterbo, *J. Appl. Crystallogr.* **1989**, *22*, 389–393.

[20] DIRDIF94. P. T. Beurskens, G. Admiraal, G. Beurskens, W. P. Bosman, R. de Gelder, R. Israel, J. M. M. Smits, The DIRIF94 program system, Technical Report of the Crystallography Laboratory, University of Nijmegen, The Netherlands, **1994**.

[21] Hai-Fu Fan, Structure Analysis Programs with Intelligent Control, Rigaku Corporation, Tokyo, Japan, **1991**.

[22] A. Altomare, M. C. Burla, M. Camalli, M. Cascarano, C. Giacovazzo, A. Guagliardi, G. Polidori, *J. Appl. Crystallogr.* **1994**, *27*, 435.

Received: May 28, 2007
Published Online: August 17, 2007

